

Block Copolymers Derived from Azobiscyanopentanoic Acid. XI. Properties of Silicone-PMMA Block Copolymers Prepared via Polysiloxane(azobiscyanopentanamide)s

HIROSHI INOUE, AKIRA UEDA, and SUSUMU NAGAI, *Osaka Municipal Technical Research Institute, 1-6-50, Morinomiya, Joto-ku, Osaka 536, Japan*

Synopsis

Mechanical, thermal, and surface properties of poly(dimethylsiloxane)-poly(methyl methacrylate) block copolymers (PDMS-*b*-PMMA) prepared by the use of polysiloxane(azobiscyanopentanamide)s were intensively investigated. The mechanical strength of block copolymers was found to decrease with an increase of siloxane contents. Dynamic mechanical analysis (DMA) of block copolymers having long siloxane chain length (SCL) and high siloxane content revealed the existence of two glass transitions attributable to microphase separation of two segments. Differential scanning calorimetry (DSC) also gave some evidence of microphase separation supporting the DMA results. It was observed that the incorporation of PDMS segments in block copolymers improved thermal stability of PMMA, as confirmed by thermogravimetric analysis. Surface analysis of the block copolymers films cast from several solutions indicated surface accumulation of PDMS segments, as revealed by water contact angle and ESCA measurements.

INTRODUCTION

In our previous paper,¹ macroazoinitiators containing polysiloxane segments, i.e., poly(azo-containing siloxaneamide)s, hereafter abbreviated as PASAs, were proposed to be interesting intermediates useful for synthesis of silicone-vinyl block copolymers including ordinary vinyl monomers capable of radical polymerization. The PASAs were found to behave as effective radical initiators for vinyl monomers comparable to α, α' -azobisisobutyronitrile (AIBN), as well as polymerization with poly(azobiscyanopentanamide)s²⁻⁴ and poly(azobiscyanopentanoate)s.⁵⁻⁷

The degree of condensation in PASAs varied ranging from 2 to 32, depending on siloxane chain length (SCL), purity of reagents, and polycondensation conditions. Therefore, there is a high probability that a mixture of A-B, ABA, BAB, and/or (A-B)_n multiblock copolymers for polysiloxane (A) and vinyl polymer segments (B) can be formed by polymerization of vinyl monomers by PASA, depending on the termination mechanism and chain transfer constants of propagating radicals.

In this work, the mechanical, thermal, and surface properties of polydimethylsiloxane-poly(methyl methacrylate) block copolymers (PDMS-*b*-PMMA) prepared via PASAs were intensively investigated focusing on effect of PDMS segments.

EXPERIMENTAL

Materials

The synthesis of PDMS-*b*-PMMA was performed by the use of several PASAs as macroazoinitiators, as described in the preceding paper.¹ The solvents used were special or first grades of commercial products without further purification.

Analysis of PDMS-*b*-PMMA

¹H-NMR spectra were measured with a JEOL NMR spectrometer FX-90 (90 MHz) using DCCl₃ solution at 50°C to determine the siloxane contents in mol %.

Molecular weights and their distributions were determined by gel permeation chromatography (GPC) using Waters liquid chromatograph 150-C. The measurement conditions were as follows: detector refractive index; columns Shodex 80M, 80M and 802.5 in this series; eluent tetrahydrofuran (THF); elution rate 1 mL/min; temperature 40°C; pressure 32 bars. The molecular weights were calibrated with polystyrene standards (Pressure Chemical Co.).

Mechanical Property Measurement

Tensile stress-strain behavior was observed using a Shimadzu Autograph DSS-5000 at 23°C and 50% RH with a crosshead speed of 5 mm/min. Hot-pressed sheets, 0.5 mm in thickness, were stamped using a die modified from JIS, into dumbbell forms having 5 mm width and 20 mm chuck distance. Two or three measurements were averaged.

Dynamic mechanical analysis (DMA) was done at 10 Hz using a Iwamoto viscoelastic spectrometer VES-S and a data processor. The specimens of 5 mm width, 50 mm length, and 2 mm thickness made by compression molding were analyzed at heating rate of 2°C/min from -150 to ca. 160°C or 1°C/min from room temperature to ca. 160°C.

Thermal Analysis

Differential scanning calorimetry (DSC) of block copolymer powders purified by reprecipitation technique was performed by a Rigaku thermal analyzer DSC 8230 and a data processor. The analysis was done from -150°C to 170°C at heating rate of 10°C/min in a nitrogen stream.

Thermogravimetric analysis (TG) was made with a Shimadzu microbalance RMB-50 in streams of nitrogen gas and air, where 10 mg of powdery samples were heated at a rate of 10°C/min.

Surface Analysis

Water contact angles of ca. 0.1 mm-thick films made by solution casting were measured with an Erma contact angle meter, Model II at 23°C and 50% RH. All measurements on both air and glass sides were conducted after 2 min of placing drops on the cast films.

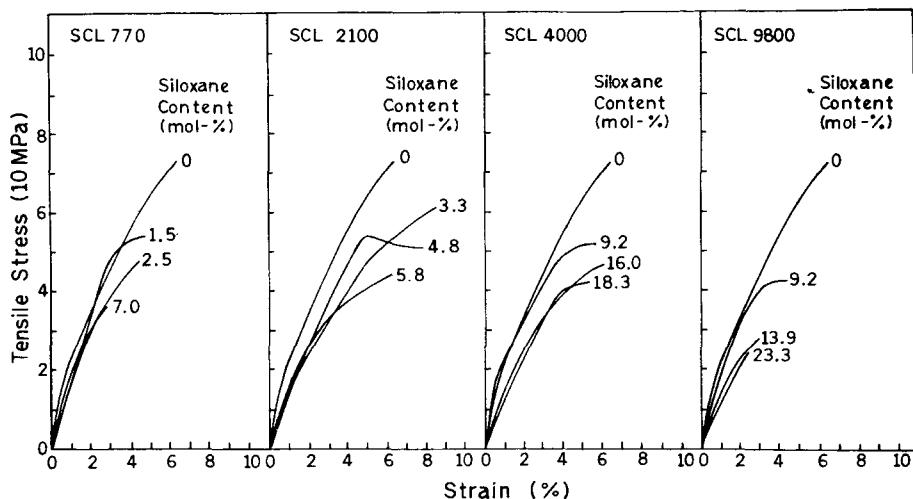


Fig. 1. Tensile stress-strain curves for PDMS-*b*-PMMA containing SCL of 770, 2100, 4000, and 9800.

X-ray photoelectron spectroscopy (XPS), or electron spectroscopy for chemical analysis (ESCA), of film with a diameter of 5 mm was done using a Shimadzu X-ray photoelectron spectrometer ESCA-750 and a data processor ESCAPAC 760. A Mg anode was employed under vacuum at 2×10^{-7} torr, and applied voltage and current were 6 kV and 30 mA, respectively. All aliphatic carbon 1s peaks were assigned to a binding energy of 285.0 eV to correct the energy shift due to electrification. Normalized ESCA peak intensity was obtained by dividing the integrated numbers of photoelectron counts in the peak area by a relative strength factor, i.e., photoelectron crosssection. The relative strength factors used here were carbon 1s 1.00, oxygen 1s 2.90, and silicon 2p 0.86.⁸

RESULTS AND DISCUSSION

Mechanical Properties of PDMS-*b*-PMMA

Tensile stress-strain curves for PDMS-*b*-PMMA are shown in Fig. 1.

This figure roughly reveals that increasing siloxane content in the copolymers results in decreasing tensile strength at break and modulus. In most cases, elongation at break tends to decrease with an increase of the siloxane content.

The effects of molecular weight, in this case, number average molecular weight (M_n), on the tensile strength at break of PDMS-*b*-PMMA are illustrated in Fig. 2. No definite tendency can be derived from this figure, although tensile strength of PMMA homopolymer is generally known to increase with an increase of molecular weight. Conversely, the plots of tensile strength against siloxane content in the same SCL series consistently showed decrease in tensile strength with increase in siloxane content, as shown in Fig. 3. Similar results were reported for silicone-styrene block copolymers,⁹

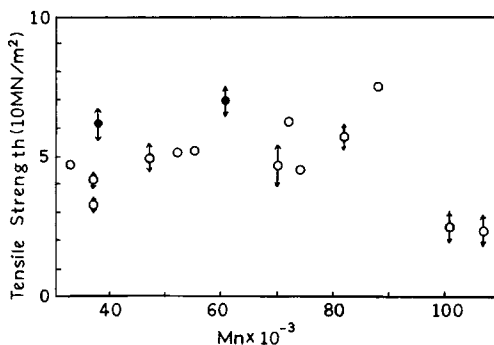


Fig. 2. Molecular weight dependence of tensile strength at break for PDMS-*b*-PMMA (○) and PMMA (●).

silicone-acrylate copolymers,¹⁰ silicone-urea acrylate copolymers,¹¹ and PMMA-PDMS block copolymers.¹²

In order to draw a conclusion regarding effect of SCL on the tensile strength, it is necessary to prepare the block copolymers having a same siloxane content. However, a difficulty of obtaining the block copolymers having the same siloxane content was met in our synthetic method. Furthermore, the siloxane content of the block copolymers prepared by our method was relatively low, in fact, less than 30 mol %. Therefore, the tensile strength was compared among the block copolymers with similar siloxane contents, for example, 7.0, 5.8, 9.2, and 9.2 mol % for SCL of 770, 2100, 4000, and 9800, respectively, in this experiment. The block copolymers with higher than 2100 of SCL, as a result, exhibited somewhat higher tensile strength and elongation than that of 770. As will be seen later, the block copolymers having an SCL of 770 consisted of a continuous phase while the others having higher SCL were recognized as phase-separated microstructure. Unexpectedly, our data did not reveal significant effects of SCL on tensile properties.

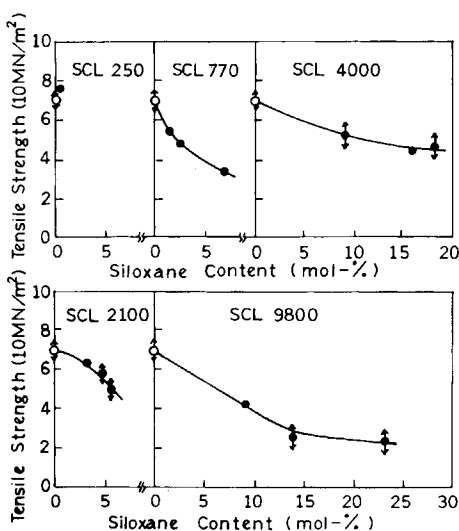


Fig. 3. Relationship between tensile strength at break and siloxane content of PDMS-*b*-PMMA.

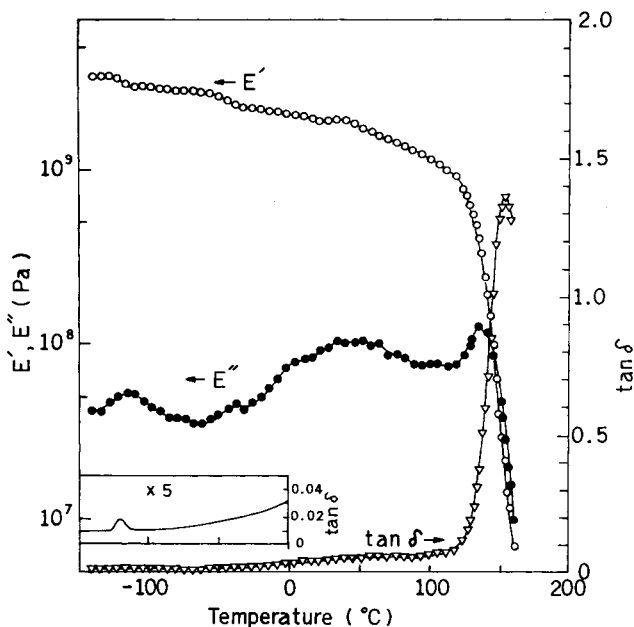


Fig. 4. Dynamic mechanical properties of SCL 9800; siloxane content 23.3%.

Fig. 4 illustrates results of dynamic mechanical analysis (DMA) of PDMS-*b*-PMMA, having an SCL of 9800 and a siloxane content of 23.3 mol %, as a typical example. This block copolymer was proved to possess two glass transition temperatures (T_g) of around -120 and 150°C from storage modulus (E') decrease and $\tan \delta$ peak, although the former T_g attributable to PDMS segments was less significant than the latter T_g attributable to PMMA segments. Thus, the presence of two T_g 's in PDMS-*b*-PMMA suggests that PDMS segment and PMMA segments are microphase-separated. In the PDMS-*b*-PMMA with lower than 23 mol % siloxane content, the DMA patterns provided insufficient information to identify the T_g of PDMS segments, probably because of relative low siloxane content and low sensitivity to

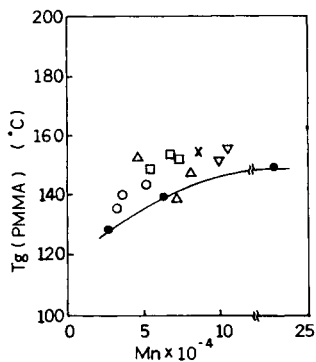


Fig. 5. Molecular weight dependence of T_g (PMMA) estimated from DMA: (●) PMMA; (X) PDMS-*b*-PMMA (SCL 250); (○) PDMS-*b*-PMMA (SCL 770); (Δ) PDMS-*b*-PMMA (SCL 2100); (□) PDMS-*b*-PMMA (SCL 4000); (∇) PDMS-*b*-PMMA (SCL 9800).

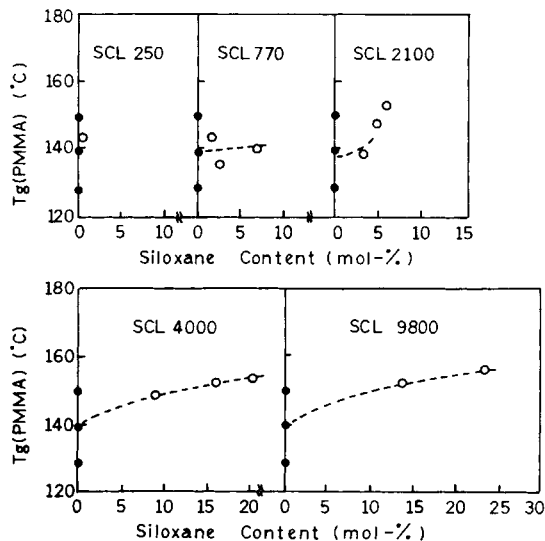


Fig. 6. Relationship between T_g (PMMA) and siloxane content (dynamic mechanical analysis).

tan δ change. In contrast, the T_g of PMMA segments, abbreviated as $T_{g(\text{PMMA})}$, was readily identified, varying slightly with molecular weights M_n and siloxane contents. The plots of $T_{g(\text{PMMA})}$ against M_n are shown in Fig. 5. This figure shows that $T_{g(\text{PMMA})}$ is slightly higher than that of MMA homopolymers having similar molecular weights. In addition, as can be seen from Fig. 6, $T_{g(\text{PMMA})}$ increases slightly with an increase of siloxane content in the same SCL series. These glass transition phenomena can be interpreted in terms of microphase separation of the segments and specific interaction between amide group and PMMA ester group through hydrogen bonding. The effects of SCL on $T_{g(\text{PMMA})}$, however, were scattered in our data and could not be further interpreted. T_g variation in hard segments was also reported on several copolymers,^{10,11} and ascribed to specific interactions.

Thermal Properties of PDMS-*b*-PMMA

Differential scanning calorimetry (DSC) was made for those PDMS-*b*-PMMA powders. Typical DSC thermograms for MMA homopolymer and block copolymers with a wide range of SCL are shown in Fig. 7. T_g was determined from thermograms as intercepts of two asymptotes.

In DSC curves, PDMS-*b*-PMMA having a SCL of 2100 or higher, exhibited two T_g 's around -125 and 140°C , which are attributed to the PDMS segments and the PMMA segments, respectively, suggesting the higher sensitivity of DSC for detecting the T_g than that of DMA. Furthermore, in the case of PDMS-*b*-PMMA with a SCL of 9800 (ca. 130 Si units) and a high siloxane content, crystallization at around -100°C and melting at around -40°C were observed in the DSC scans. This probably indicates structural change in the PDMS segment caused by SCL increase, actually, higher than 4000.

PDMS-*b*-PMMA having shorter SCL (770 or 250) did not exhibit any detectable lower T_g , but almost the same thermogram as that of the MMA

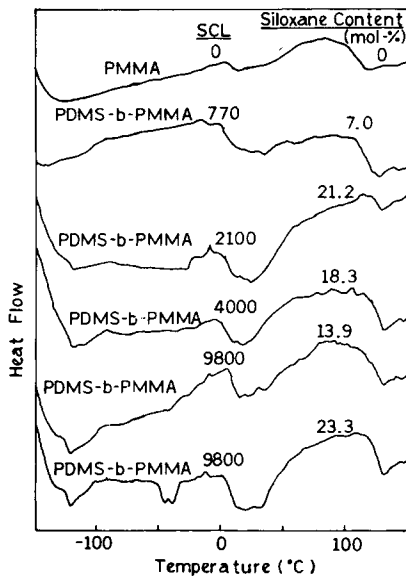


Fig. 7. DSC traces of PMMA and PDMS-*b*-PMMA in N₂. Heating rate 10°C/min.

homopolymer. The solution-cast films of these samples were transparent while those of PDMS-*b*-PMMA having longer SCL were translucent. This indicates that the PDMS-*b*-PMMA having shorter SCL consists of a homogeneous phase.

Of interest here is that there exists a critical SCL that exhibits transition from homogeneous to heterogeneous phases at around 1000, that is, between 770 and 2100. The SCL which is longer than the critical one has little effect on the lower T_g of PDMS segments, at a nearly constant temperature, -125°C. On the contrary, the upper T_g , at around 120°C varied slightly with SCL, siloxane content, and M_n . Molecular weight dependence of $T_{g(\text{PMMA})}$ measured by DSC is shown in Fig. 8. The $T_{g(\text{PMMA})}$ for PDMS-*b*-PMMA was found to be constantly higher than those of MMA homopolymers, agreeing with the DMA results mentioned above. This may be attributed to distinct microphase separation and specific interaction between amide group and PMMA ester group in the PDMS-*b*-PMMA, and is significantly different from the DSC results in styrene-dimethylsiloxane diblock copolymers.¹³ It was observed

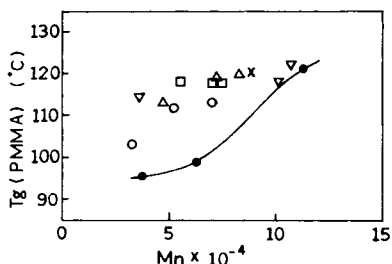


Fig. 8. Molecular weight dependence of T_g (PMMA) evaluated from DSC: (●) PMMA, (X) PDMS-*b*-PMMA (SCL 250); (○) PDMS-*b*-PMMA (SCL 770); (Δ) PDMS-*b*-PMMA (SCL 2100); (□) PDMS-*b*-PMMA (SCL 4000); (▽) PDMS-*b*-PMMA (SCL 9800).

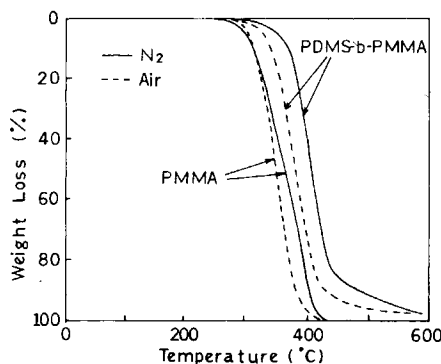


Fig. 9. Thermogravimetric analysis of PMMA and PDMS-*b*-PMMA. Heating rate 10°C/min. PMMA; $M_n = 112,000$, $M_w = 103,000$. PDMS-*b*-PMMA: $M_n = 107,000$, $M_w = 676,000$. SCL = 9800; siloxane content = 23.3 mol %.

that the T_g of PMMA phase approaches those of MMA homopolymers with an increase of M_n .

This T_g variation for the hard PMMA segment is significantly different from those of silicone-acrylate,¹⁰ silicone-urea acrylate,¹¹ and silicone-poly-carbonate block copolymers,¹⁴ containing partially mixed phases. Thermogravimetric analysis (TG) is important to assess thermal stability of these types of silicone-PMMA block copolymers having little residual azo group.

Fig. 9 shows the TG curves for PDMS-*b*-PMMA with an SCL of 9800 and a siloxane content of 23.3 mol % in air and nitrogen atmospheres as a typical example. As can be seen from this figure, this block copolymer started to degrade at approximately 250–270°C, suggesting relatively high thermal stability and almost no residual azo group. After compression molding at 200°C for preparing DMA specimens, the PDMS-*b*-PMMA sample described in Fig. 4 was examined for GPC molecular weight determination to evaluate the effect of thermal history. As a result, the molecular weight of the PDMS-*b*-PMMA sample (originally, $M_n = 107,000$, $M_w = 676,000$, and $M_w/M_n = 6.31$) decreased slightly to $M_n = 80,000$, $M_w = 312,000$, and $M_w/M_n = 3.90$. Therefore, the thermally scissile azo group appears to be almost totally consumed during the radical polymerization to form the block copolymer. Several PDMS-*b*-PMMA samples were found to start degradation at temperatures lower than 200°C, suggesting that the presence of the residual azo group in PDMS-*b*-PMMA cannot be neglected in these samples.

In Fig. 9, it is also characteristic that PDMS-*b*-PMMA both in air and nitrogen atmospheres shows good thermal stability, 30–50°C higher than MMA homopolymers with a similar molecular weight. This is attributed to incorporation of PDMS segment into PMMA.

In this experiment, the onset temperatures for thermal decomposition were hardly identified from their thermogravimetric curves. In addition, stepwise decomposition patterns in any curves were not detected. Therefore, 5%-decomposition temperature, for the simplicity, was taken as an index to assess thermal stability, instead of onset temperature for thermal decomposition. Effect of siloxane content on the 5%-decomposition temperatures of PDMS-*b*-PMMA measured in nitrogen atmosphere is illustrated in Fig. 10.

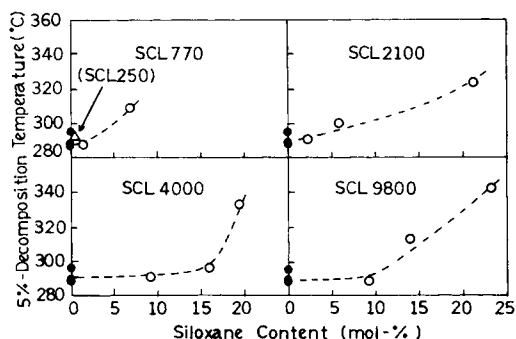


Fig. 10. Relationship between 5%-decomposition temperature and siloxane content of PDMS-*b*-PMMA in N_2 atmosphere. Heating rate $10^\circ\text{C}/\text{min}$.

This figure reveals that, in the PDMS-*b*-PMMA having siloxane content of more than ca. 10 mol %, 5%-decomposition temperature was evidently $30\text{--}50^\circ\text{C}$ higher than that of MMA homopolymers in all the SCL series, as a result of incorporation of PDMS chain. A similar tendency for TG was also reported for styrene-siloxane block copolymers made by living anionic initiators.¹⁵

Surface Properties of PDMS-*b*-PMMA

It is well known that PDMS exhibits excellent hydrophobicity, as evaluated from water contact angle, and that PDMS segments occupy the outermost surfaces of PDMS-polystyrene, and -PMMA block copolymer films, as demonstrated by contact angle^{12,16,17} and ESCA measurements.¹⁷ These two techniques were applied to our block copolymer systems.

Three kinds of solvents, benzene, methylene chloride, and methylethylketone, were used to make solution-cast films for water contact angle measurements (dipole moment: benzene 25°C , 2.275; methylene chloride 25°C , 8.93; methylethylketone 20°C , 18.51).¹⁸ The contact angles were plotted against the siloxane contents of block copolymers having SCL of 2100, as illustrated in Fig. 11. A commercial PDMS with a medium viscosity was confirmed to have a water contact angle of ca. 95° in our measurement conditions. Therefore, this figure shows that the outermost surface of the solution-cast films, particularly on the air side, consists predominantly of PDMS segments in more than 1 mol % of bulk siloxane contents. Also, it is interesting to note that the difference in contact angles between surfaces on air side and glass side of some films appears in a region of lower siloxane contents. Polar solvents like methylethylketone and methylene chloride were found to be significantly effective in inducing the contact angle difference between the sides. Surface accumulation of PDMS segment even in very low siloxane contents is essentially ascribed to microphase separation of the segments, and, similarly, to a certain surface energy difference between the segments. Glass with high surface energy as a hydrophilic extreme is a clear contrast with air as an imaginary hydrophobic extreme. Therefore, the hydrophobic air side prefers the PDMS segment over PMMA segments, when more polar solvents are used for casting. On the other hand, neither side of the films exhibited significant difference in contact angles, when a nonpolar solvent like benzene was used for casting.

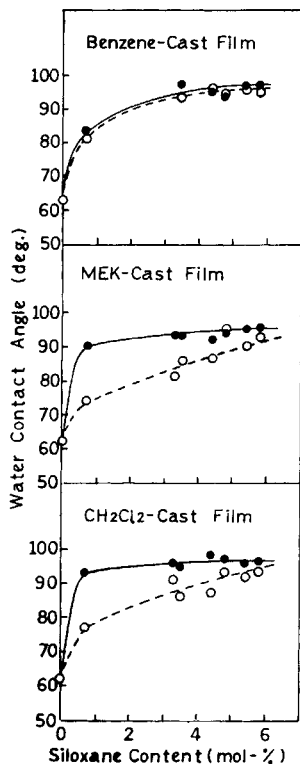


Fig. 11. Relationship between water contact angles and siloxane contents of PDMS-*b*-PMMA with an SCL of 2100: (●) air side; (○) glass side.

ESCA spectra, which provide information with regard to surface abundance of each element from the topmost ca. 50 Å, were measured to confirm surface accumulation of the PDMS segments. Typical examples for ESCA spectra of several block copolymer films are shown in Fig. 12.

On the air side surface of benzene cast films of PDMS-*b*-PMMA having a SCL of 2100, the Si_{2p} peaks attributable to PDMS segments abruptly increase as an increase of the siloxane content. The O_{1s} and C_{1s} peak patterns at a siloxane content of only 5.8 mol % were almost the same as those of pure PDMS. At this siloxane content, both the Si_{2p}/C_{1s} and O_{1s}/C_{1s} intensity ratios, normalized with the photoelectron crosssections, correspond to almost 0.5, the theoretical values of PDMS segments. The Si_{2p}/C_{1s} ratios of both sides of the films cast from benzene and methylethylketone solutions are plotted against the siloxane contents of the PDMS-*b*-PMMA, as shown in Fig. 13.

It was observed that Si_{2p}/C_{1s} intensity ratio, as an index of surface abundance of PDMS segments, abruptly increases on both sides with an increase of siloxane contents, although the data moderately scatter, particularly, in the films cast from methylethylketone solutions. It was also noted that molar fractions of PDMS segments on outermost surface, estimated from Si_{2p}/C_{1s} intensity ratios, increased to over 80 mol % even in very low bulk

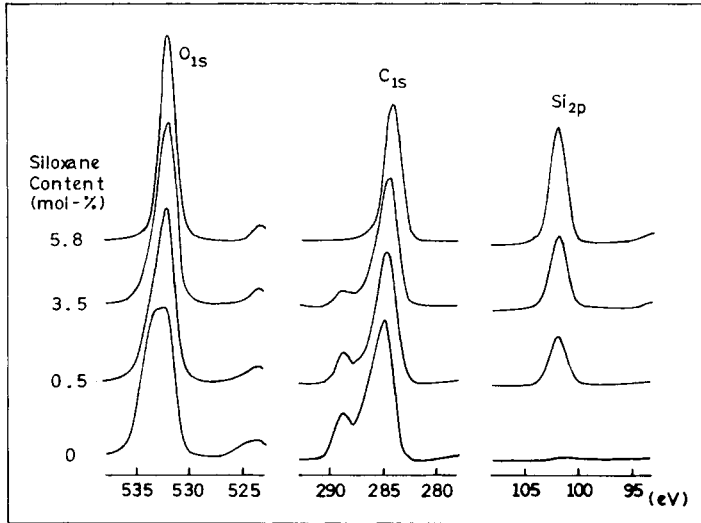


Fig. 12. ESCA spectra of PDMS-*b*-PMMA films cast from benzene solution on glass plate (air side).

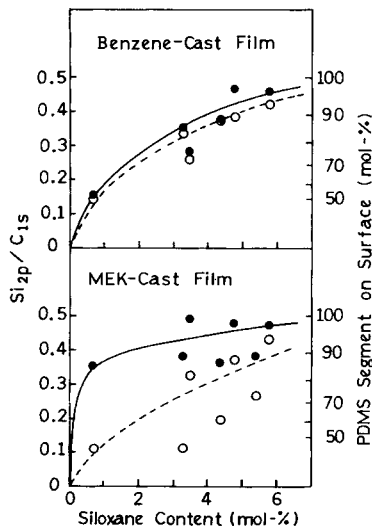


Fig. 13. Relationship between ESCA $\text{Si}_{2p}/\text{C}_{1s}$ ratios and siloxane contents of PDMS-*b*-PMMA with an SCL of 2100: (●) air side; (○) glass side.

siloxane content. This was calculated on the assumption of nearly equal escape depth of each photoelectron similar to that of PDMS-polystyrene diblock copolymers.¹⁷ Furthermore, it is significantly noteworthy that critical difference of solvent polarity between benzene and methylethylketone results in the difference of surface abundance of segments between air and glass sides. Thus, benzene has no significant effect on the difference in surface abundance of PDMS segments between the two sides. Conversely, methylethylketone polarity causes energy difference between air-copolymer and glass-copolymer

interfaces, indicating that polar PMMA segments tend to orient to the glass surface, and vice versa. This surface behavior is confirmed by water contact angle measurement, as described above.

Electron probe microanalysis for fractured surfaces was examined to confirm this surface accumulation behavior of PDMS segments. However, this failed to detect Si atom distribution through the fractured surfaces with sufficient sensitivity.

CONCLUSIONS

In this work, some properties of silicone-PMMA multiblock copolymers prepared by means of radical polymerization of methyl methacrylate in the presence of poly(azo-containing siloxaneamide)s (PASAs) were intensively studied. The mechanical strength, as evaluated from tensile strength, decreased with an increase of siloxane contents, primarily due to low mechanical strength of PDMS, which became the break points on deformation, and microphase separation. Dynamic mechanical analysis (DMA) suggests the presence of microphase separation, particularly, in longer SCL. T_g variation dependent on siloxane content, explained in terms of microphase separation and specific interaction between amide group and PMMA ester groups and supported by DSC data, is of interest here. Multiple transitions of PDMS-based acrylates and methacrylates^{10,11,19,20} are already known to ascribe to the development of microphase separation. In our systems, a critical SCL was recognized at 770–2100, i.e., 9–27 Si units, to vary from miscible to microseparated phase. Incorporation of PDMS segments into PMMA brought about heat-resistant properties, as revealed from thermal degradation of PDMS-*b*-PMMA, although residual azo groups on the polymer chains were labile to heating.

Specific surface properties, such as water repellency and, furthermore, release properties, were observed in these PDMS-*b*-PMMA films. Surface accumulation of PDMS segments, particularly on the air sides, was confirmed by water contact angles and ESCA spectra, depending on siloxane content. These phenomena imply useful application of PDMS-vinyl block copolymers to surface modifiers.

References

1. H. Inoue, A. Ueda, and S. Nagai, *J. Polym. Sci., Polym. Chem. Ed.*, to appear.
2. A. Ueda, Y. Shiozu, Y. Hidaka, and S. Nagai, *Kobunshi Ronbunshu*, **33**, 131 (1976).
3. A. Ueda and S. Nagai, *J. Polym. Sci., Polym. Chem. Ed.*, **22**, 1783 (1984).
4. A. Ueda and S. Nagai, *J. Polym. Sci., Polym. Chem. Ed.*, **22**, 1611 (1984).
5. A. Ueda, Y. Hidaka, and S. Nagai, *Kobunshi Ronbunshu*, **36**, 123 (1979).
6. A. Ueda and S. Nagai, *J. Polym. Sci., Polym. Chem. Ed.*, **24**, 405 (1986).
7. A. Ueda and S. Nagai, *Kobunshi Ronbunshu*, **43**, 97 (1986).
8. J. H. Scofield, *J. Electron Spectrosc.*, **8**, 129 (1976).
9. J. V. Crivello, J. L. Lee, and D. A. Conlon, *J. Polym. Sci., Polym. Chem. Ed.*, **24**, 1251 (1986).
10. T. R. Williams, *J. Appl. Polym. Sci.*, **31**, 1293 (1986).
11. X. Yu, M. R. Nagarajan, C. Li, T. A. Speckhard, and S. L. Cooper, *J. Appl. Polym. Sci.*, **30**, 2115 (1985).

12. S. K. Varshney and C. L. Beatty, *Org. Coat. Plast. Chem.*, **45**, 152 (1981).
13. S. Krause, M. Iskandar, and M. Iqbal, *Macromolecules*, **15**, 105 (1982).
14. T. C. Ward, D. P. Sheehy, J. S. Riffle, and J. E. McGrath, *Macromolecules*, **14**, 179 (1981).
15. P. Bajaj, S. K. Varshney, and A. Misra, *J. Polym. Sci., Polym. Chem. Ed.*, **18**, 295 (1980).
16. G. L. Gaines, Jr. and G. W. Bender, *Macromolecules*, **5**, 82 (1972).
17. D. T. Clark, J. Peeling, and J. M. O'Malley, *J. Polym. Sci., Polym. Chem. Ed.*, **14**, 543 (1976).
18. J. A. Riddick and W. B. Bunger, *Organic Solvents*, 3rd. ed., Wiley-Interscience, New York, 1970.
19. D. Katz and I. G. Zewi, *J. Polym. Sci. C*, **46**, 139 (1974).
20. D. Katz and I. G. Zewi, *J. Polym. Sci., Polym. Chem. Ed.*, **16**, 567 (1978).

Received August 28, 1987

Accepted September 2, 1987